DOI: 10.1002/ejic.200900803

Origin of the Paramagnetic Properties of the Mixed-Valence Polyoxometalate $[GeV_{14}O_{40}]^{8-}$ Reduced by Two Electrons: Wave Function Theory and Model Hamiltonian Calculations

N. Suaud,*[a] Y. Masaro,[a] E. Coronado,[b] J. M. Clemente-Juan,[b] and N. Guihéry[a]

Keywords: Polyoxometalates / Mixed-valent compounds / Ab initio calculations / Electron transfer / Magnetic properties

The aim of the work is to give an explanation of the magnetic properties of a mixed-valence $[GeV_{14}O_{40}]^{8-}$ polyoxometalate reduced by two electrons, which, in contrast to what happens in other two-electron-reduced polyoxometalates, does not show any magnetic coupling between the two unpaired electrons. For this purpose, a quantitative evaluation of the microscopic electronic parameters (electron transfer, magnetic coupling, magnetic orbital energy, and Coulomb repulsion) of the mixed-valence polyoxometalate cluster is performed. The parameters are extracted from valence-spectroscopy large configuration interaction (CI) calculations on embedded fragments. Then, these parameters are used in an extended *t-J* model Hamiltonian suited to model the properties of the whole anion. The analysis of the wave functions of the lowest singlet and triplet states and of the microscopic parameters emphasizes that the electron delocalization in this mixed-valence cluster is such that each unpaired electron is almost trapped in a different half of the polyoxovanadate, thus disabling any exchange interaction between them.

1 Introduction

Polyoxometalates (POMs) are a class of metal oxide compounds mainly based on V, Mo, and W ions in their highest oxidation states. They present a remarkable degree of molecular and electronic tunability that have an impact in many disciplines (catalysis, medicine, materials science).[1–5] Due to their cluster-type structure, POMs are specially useful as model systems for the studies of electronic and magnetic interactions. Indeed, many of these structures allow the inclusion of paramagnetic ions with various nuclearities and definite topologies and geometries.[6] Moreover, they permit a controlled injection of electrons, giving rise to mixed-valence (MV) species in which delocalized electrons may coexist and interact with localized magnetic moments. In this context they provide unique molecular systems for the development of new theories in the MV area. An important property of POMs is that their identity is usually preserved by reversible redox processes,[7] forming reduction products known as "heteropoly blues" or "heteropoly browns" by addition of various numbers of electrons that are delocalized over the cluster.[8] This property has been often found in POMs of W and Mo based on three different structural types, namely Lindqvist (M_6), Keggin (M_{12}), and Wells–Dawson (M_{18}). In all the reported cases, however, it has been observed experimentally that the spins are completely paired in a singlet ground spin state, even at room temperature. The origin of this antiferromagnetic coupling led to a controversy, depending on whether a multiroute superexchange mechanism[9] or a mechanism involving electron delocalization and electrostatic repulsion was considered. Various theoretical approaches finally proved the validity of the second mechanism.[10–12] This model has been extended to explain the unusually strong magnetic coupling found in MV polyoxovanadates containing 10 spin electrons delocalized over 18 metal sites.[13]

In 2006, U. Kortz et al. presented the synthesis of the $[GeV_{14}O_{40}]^{8-}$ POM[14] (see Figure 1) analogous to Evans' 14-vanadoaluminate $[AlV_{14}O_{40}]^{9-}$[15] (the anionic component of the sherwoodite,[17] a natural mineral of formula $Ca_{4.5}[AlV_{14}O_{40}]$). In 1991, another analog to Evans' 14-vanadoaluminate was reported by Müller et al., $[AsV_{14}O_{40}]^{7-}$, in a paper that underlines the interest of understanding the (bio)geochemistry of vanadium.[16] The structural characterization (X-ray diffraction, NMR, IR, UV/Vis) and electrochemical and magnetic properties (magnetic susceptibility, EPR, XPS) of $(K_2Na_6[GeV_{14}O_{40}]\cdot 10H_2O)$ crystals of point group D_{2h} were reported. The oxidation state of this compound corresponds to the existence of twelve V^V and two V^{IV} cations. From a bond valence sum (BVS) analysis, Kortz et al. concluded that the two "extra" electrons are essentially localized, explaining why this compound is, to the best of our knowledge, the only paramagnetic two-electron-reduced POM. It is therefore interesting to study in detail its electronic structure to get a

[a] Laboratoire de Chimie et Physique Quantiques, IRSAMC, Université de Toulouse and UPS, CNRS, UMR 5626, 31062 Toulouse, France
E-mail: suaud@irsamc.ups-tlse.fr
[b] Instituto de Ciencia Molecular, Universidad de Valencia, Polígono de la Coma, s/n 46980 Paterna, Spain

better understanding of the origin of its magnetic properties. For this purpose we used a methodology already used for other POMs,[12] namely: (i) evaluation of the relevant microscopic parameters (electron transfer, magnetic coupling, orbital energy, and electrostatic repulsion) by using large CI calculations on embedded fragments; (ii) introduction of these values in a model Hamiltonian suited to reproduce the properties of the whole compound, extraction of the energy spectrum, wave functions, and simulation of the magnetization curve.

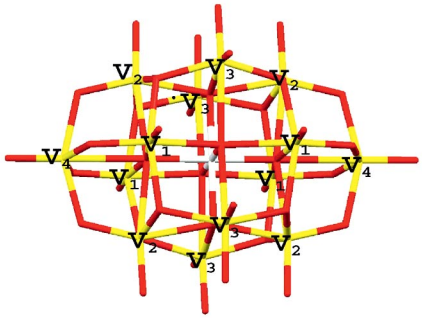

Figure 1. Structure of the $[GeV_{14}O_{40}]^{8-}$ anion. The V cations are shown in yellow, the oxygen anions in red, and the central Ge ion in white.

The manuscript is organized as follows: section 2 provides a brief description of the structure of the $[GeV_{14}O_{40}]^{8-}$, section 3 details the embedded fragment calculation method, presents the model Hamiltonian used, and describes the method of extraction of parameters from effective Hamiltonians, section 4 is dedicated to the presentation of the results and to the discussion, and the conclusion is given in section 5.

2 Structure of the Compound

The X-ray structure[14] shows that the V ions are arranged at the surface of an ellipsoid (the long and short axes are about 8.5 Å and 6.6 Å, respectively). They are distributed on parallel planes perpendicular to the long axis: the four V_3 vanadium ions are in the central plane containing the Ge atom, four vanadium ions (V_1 and V_2) are on each of the two planes at a distance of about 2.1 Å from the central one and one vanadium (V_4) on each of the farthest planes (4.3 Å from the central one). Vanadium ions are inside distorted octahedra formed by six oxygen ions. For V_1, V–O distances are 1.61 Å to the apical oxygen atom (the one that points outside the molecule), 1.72 Å to oxygen atoms bridging toward V_4, 1.95 Å to each oxygen atom bridging toward V_2 atoms, 2.17 Å to the oxygen atom of the V_3 plane, and 2.31 Å to the oxygen atom inside the ellipsoid. Although V_1 and V_2 are not symmetrically equivalent, they are inside very similar octahedra: the V_2–O distances are 1.61 Å, 1.72 Å, 1.96 Å, 2.14 Å, and 2.29 Å. The differences between V_1 and V_2 are due to the position of the Na^+ and K^+ counterions (not represented in Figure 1). The V_4–O bond lengths are 1.60 Å to the apical oxygen atom, 1.94 Å to the oxygen atom bound to V_1, 1.95 Å to the oxygen atom bound to V_2, and 2.40 Å to the oxygen atom inside the complex. The octahedra containing V_3 are clearly different. V_3 has two apical oxygen atoms (bond lengths are 1.64 Å) and forms two bonds of 1.92 Å with the oxygen bridging toward V_1 and V_2 and two bonds of 2.33 Å and 2.39 Å with the oxygen bridging with the other V_3. According to the Pope classification,[8,18] V_1, V_2, and V_4 are of type I, whereas V_3 are of type II.

For the further discussion, it is useful to conceive the POM as two square-based pyramids (containing V_1, V_2, and V_4 atoms) separated by the plane formed by the V_3 atoms.

3 Model Hamiltonians, Embedded Fragment Calculations, and Extraction of Microscopic Parameters

3.1 Model Hamiltonian

In reduced POMs, the unpaired "extra" electrons are essentially delocalized over the V d_{xy}-like orbitals (defining for each VO_6 octahedron a z axis as the V–O_{apical} direction) that point in between the equatorial O ions of the octahedron. Hence, a model Hamiltonian suited to describe the magnetic properties of a reduced anion has to take into account the main effective interactions between the electrons in these orbitals. These are: the magnetic exchange interactions, J_{ij}, the electron-transfer hopping integrals between orbitals i and j, t_{ij}, the orbital energy, ε_i, and the electrostatic repulsions between the two electrons, V_{ij}, on different sites. The model Hamiltonian can be written as follows:

$$H = \Sigma_i \varepsilon_i n_i + \Sigma_{<i,j>} t_{ij} \Sigma_\sigma (c^\dagger_{i_\sigma} c_{j_\sigma} + c^\dagger_{j_\sigma} c_{i_\sigma}) - \Sigma_{<i,j>} J_{ij} (\vec{S}_i \vec{S}_j - \tfrac{1}{4} n_i n_j) + \Sigma_{(i,j)} V_{ij} n_i n_j$$

where the sum over i runs over the d_{xy}-like orbitals of all V centers, the sum over $<i,j>$ runs over all nearest-neighbor V d_{xy}-like pairs, the sum over (i,j) runs over all V d_{xy}-like pairs, $\vec{S}_i$ is the local spin operator on site i, $c^\dagger_{i_\sigma}$ and c_{i_σ} are the usual creation and annihilation operators, respectively, of an electron of spin σ on site i, n_i is the number operator on site i. This model Hamiltonian operates on all the configurations generated by spreading a given number of "extra" electrons over a given number of metal center orbitals (2 electrons and 14 orbitals for the two-electron-reduced V14) except those where two "extra" electrons occupy the same orbital. Thus, it does not explicitly take into account the on-site electrostatic repulsion. In fact, the large value of the on-site electrostatic repulsion relative to the inter-site electrostatic repulsion is responsible for the small weight of these configurations in the low-energy wave functions.

Furthermore, the model Hamiltonian does treat the effects of such configurations through the effective value of the magnetic exchange *J* integrals.

3.2 Embedded Fragment Calculations

The exchange, hopping and electrostatic repulsion integrals are essentially local parameters.[22] Therefore, they can be accurately evaluated by using ab initio spectroscopy calculations on fragments if two conditions are met: (i) the fragments include all the short range effects, that is, the full coordination sphere of the magnetic atoms, and (ii) the long-range effects are taken into account by means of an appropriate bath reproducing the main effects of the environment.

The embedded fragment calculation method fulfills these conditions,[22,23] and its validity for MV POMs is well established.[12] The model considers: (i) a fragment based on metal centers and all the atoms of their coordination sphere, (ii) an embedding of point charges and total ion pseudopotentials (TIPs). In the fragment, the interactions between the atoms are explicitly taken into account in ab initio calculations. The aim of the embedding is to reproduce the main effects of the rest of the crystal onto the fragment, that is the Madelung field and the Pauli exclusion effects. The Madelung field is modeled by a very large set of point charges around the fragment. TIPs, encapsulating the point charges, reproduce the Pauli exclusion, avoiding an excessive polarization of the electrons of the fragment toward positive charges. The treatment of the embedding is almost computationally costless. The X-ray crystallographic structure of the compound was used in all calculations for establishing the positions of the atoms of the fragment and of the point charges of the embedding.

DFT calculations of complete POM ions are an alternative to embedded fragment calculations. They provide important information about the structure, spectrum, dynamics, and catalytic and magnetic properties[19] of isolated or solvated POMs, even for POMs including lanthanide ions.[21] Nevertheless, the extraction, from DFT calculations, of the intensity of the microscopic parameters important for the magnetic properties of POMs is difficult. Indeed, it should require the calculation of many determinants, eventually of Broken Symmetry,[20] whose convergency is tricky. As these microscopic parameters are necessary not only to reproduce the magnetic properties of a whole POM but also to understand the origin of these properties, DFT calculations are not a useful alternative to the first step (ab initio calculations) of our two-step procedure.

3.3 Ab Initio Calculations

All dimers based on VO_6 octahedra sharing at least one O ion were built and embedded in an appropriate bath of charges and TIPs. For each, we performed both CASSCF (using the MOLCAS suite of programs[24]) and DDCI[25] (using the CASDI suite of programs[26]) calculations.

According to the physics of MV compounds that permits to differentiate between orbitals depending on their contribution to electron transfer, the CASSCF procedure divides the molecular orbitals into three subspaces: (i) the doubly occupied *inactive orbitals*; (ii) the *active orbitals*, whose occupation is allowed to change; (iii) the unoccupied *virtual orbitals*.

The Complete Active Space (CAS) is then defined as the set of all the Slater determinants that can be built according to the previous occupation rules (for a given number of active electrons occupying the active orbitals). The CASSCF method optimizes self-consistently all the orbitals and all coefficients of the wave function spanned on the CAS. Polarization and correlation of the active electrons are thus *variationally* taken into account in the *mean field* of the electrons of the inactive orbitals.

Difference Dedicated Configuration Interaction[25] (DDCI) is considered as the most accurate method for the determination of effective electronic interactions in such large systems. The dynamic polarization and correlation effects are taken into account *variationally* by selecting only those configurations that contribute (at the second order of perturbation) to the energy *differences* between the states of the CAS. This method requires the diagonalization of the Hamiltonian matrix expressed in the DDCI space generated by all the single and double excitations on all the determinants of the CAS except the 2-hole-2-particle excitations. These excitations are the most numerous ones and, if we only consider energy differences, these out-of-space excitations can be ignored when a common set of molecular orbitals (MOs) are used for all the calculations.[25] All the calculations were thus performed on the set of MOs optimized at the CASSCF level for the lowest triplet state.

In our system, the active orbitals are the d_{xy}-like orbital of the V ions. The CAS is based on one electron and two orbitals for *t* and *ε* extraction. Its size is 2 and the size of the corresponding DDCI space is approximately 2.5×10^6. The projection of the DDCI wave functions onto the CAS is around 70%. For *J* extraction, the CAS is based on two electrons and two orbitals. Its size is 4, the size of the corresponding DDCI space is around 5.3×10^6, and the projection of the DDCI wave functions onto the CAS is around 90%.

The extraction of the effective electrostatic repulsions from similar ab initio calculations are much more complex, as it requires trimer calculations and/or calculations on well-separated VO_6 octahedra. Fortunately, we have shown in previous studies on POMs[12] that the $1/r$ Coulombic law taking into account only the electron–electron *r* distance is a correct approximation of the electrostatic repulsion of delocalized electrons in POMs.

In all the calculations, the inner-core electrons ($[1s^2 2s^2 2p^6 3s^2]$ for the V atoms and $[1s^2]$ for the O atoms) are represented by effective core potentials (ECP). The outer-core and valence electrons are represented by using a 9s6p6d primitive basis set contracted to 3s3p4d for the V

and a 5s6p1d primitive basis set contracted to 2s3p1d for the O atoms. Exact expressions of the basis sets and ECP can be found in ref.[27]

3.4 Effective Hamiltonian Procedure

The evaluation of the microscopic interactions of a model Hamiltonian[28] is based on calculations of the low-energy spectrum of embedded fragments and on the use of effective Hamiltonian techniques. As shown in previous papers,[12,29] the two most important points that satisfy the effective Hamiltonian are: (i) its eigenvalues are the eigenvalues of the exact Born–Oppenheimer Hamiltonian; (ii) its eigenvectors are the projections of the eigenvectors of the exact Hamiltonian onto the model space (the space handled by the effective Hamiltonian).

A Boys-based localization procedure[30,31] was performed, and localized orbitals were obtained for each fragment. Then, from the energy and wave function (decomposed on local orbitals) of the two lowest doublet states obtained from one-electron-in-two-orbitals-CAS-based calculations, the effective Hamiltonian procedure permits to extract simultaneously both the energy difference, $\Delta\varepsilon$, of the two orbitals and the electron transfer, t, between these orbitals. The value of J is directly extracted from the singlet-to-triplet energy gap calculated from a CAS based on two electrons in two orbitals.

4 Results and Discussion

4.1 Values of Microscopic Parameters

The J, t, $\Delta\varepsilon$, and V values are reported in Tables 1 and 2. The strongest t and J integrals are between V_1 and V_4 and between V_2 and V_4. The smallest interactions are along V_1–V_1 and V_2–V_2 fragments (that is, between atoms of the base of a pyramid) and along V_1^l–V_1^r and V_2^l–V_2^r (that is, between atoms of the base of each pyramid). All t or J interactions involving V_3 are weak or even negligible. Concerning the Coulomb repulsion, three groups of values exist, one around 400 meV (2 values), another between 1000 and 1700 meV (6 values), and the last one around 2800 meV (5 values).

Table 1. Values of the t, J, and $\Delta\varepsilon$ parameters in the different dimers. For a fragment V_i–V_j, $\Delta\varepsilon = \varepsilon_i - \varepsilon_j$. V_3–V_3 interactions correspond to the interactions between two V_3 ions on each side of the plane containing the V_2 ions, V_3–V_3' interactions correspond to the interactions between two V_3 ions on each side of the plane containing the V_1 ions. Superscripts l and r indicate fragments for which one vanadium ion is on the left side and the other on the right side of the plane containing the V_3 ions.

	V_1–V_4	V_2–V_4	V_1–V_2		V_1–V_3	V_2–V_3
J [meV]	–90	–167	+12		+5.2	1.3
t [meV]	–306	–463	+72		–12	+77
$\Delta\varepsilon$ [meV]	780	1453	549		2450	1828
	V_3–V_3	V_3–V_3'	V_2^l–V_2^r	V_1^l–V_1^r	V_2–V_2	V_1–V_1
J [meV]	–0.16	–8.9	–1.5	–0.65	–0.60	–0.33
t [meV]	+83	+91	–35	–19	–39	–31

Table 2. Values of the Coulombic electrostatic repulsion, V, the reference is $V_{(V_4–V_4)} = 0$ between the farthest vanadium ions. Superscripts l and r indicate fragments for which one vanadium ion is on the left side and the other on the right side of the plane containing the V_3 ions.

	V_4–V_4	V_1^l–V_4^r	V_2^l–V_4^r	V_3–V_4	V_1^l–V_2^r	V_3–V_3'	V_3–V_3
V [meV]	0	430	438	984	1010	1367	1452
	V_1–V_1	V_2–V_2	V_1–V_2	V_2–V_3	V_1–V_4	V_2–V_4	V_1–V_3
V [meV]	1688	1717	2759	2857	2897	2898	2907

Logically the sum $(\varepsilon_i - \varepsilon_j) + (\varepsilon_j - \varepsilon_k) + (\varepsilon_k - \varepsilon_j)$ should be zero. As all the $\Delta\varepsilon$ values reported in Table 1 are extracted from calculations on different dimers, a value close to zero for this sum is a check of the consistency of these calculations. For V_1–V_4, V_2–V_4, and V_2–V_1, $\varepsilon_1 - \varepsilon_4 = 780$ meV, $\varepsilon_4 - \varepsilon_2 = -1453$ meV, and $\varepsilon_2 - \varepsilon_1 = 549$ meV, resulting in a sum of –124 meV, which corresponds to an average error of less than 5% for each $\Delta\varepsilon$. The same accuracy is observed for the other fragments. It is then possible to extract the ε values minimizing the least square errors of the calculated $\Delta\varepsilon$. Table 3 compiles these values (ε_4 is chosen as zero of energy). It is clear that the magnetic orbitals lowest in energy are those of V_4, while those of V_3 are by far the highest ones. This can be rationalized by the presence of two apical oxygen atoms for V_3. The magnitude of the gap between ε_2 and ε_1 is quite surprising, since, as stated in section 1, the environments of V_1 and V_2 are very similar. This difference may be explained by the position of the Na^+ and K^+ counterions that stabilize the magnetic orbital of V_1 relative to that of V_2. Indeed, the difference of Coulombic interaction between a positive charge of each of the eight cations surrounding each POM and an electron on V_1 or on V_2 can be estimated to be 640 meV (from a $1/r$ law), which is in good agreement with the ab initio evaluation $\varepsilon_2 - \varepsilon_1 = 776$ meV.

Table 3. Values of the ε parameters.

ε_1 [meV]	ε_2 [meV]	ε_3 [meV]	ε_4 [meV]
776	1391	3256	0

4.2 Spectrum of the Whole Complex

For most of even-electron-reduced POMs, a strong stabilization of the singlet state relative to the first triplet excited state is observed. We have rationalized this behavior from the study of three POMs based on W or V ($PW_{12}O_{40}$, $W_{10}O_{32}$ and $V_{18}O_{42}$)[12] and shown that it is the consequence of strong electron transfer and strong Coulombic repulsion between the electrons. Indeed, even if the strong Coulombic repulsion keeps the "extra" electrons away from each other, a very strong effective antiferromagnetic coupling between the two spins is enabled by the complete delocalization of the electrons on the whole POM.

Then, the case of $[GeV_{14}O_{40}]^{8-}$ seems strange. Indeed, as discussed in the previous section, the electron transfer and Coulombic repulsion are of the same order of magnitude

as those for $PW_{12}O_{40}$, $W_{10}O_{32}$, or $V_{18}O_{42}$. We should then expect quite similar magnetic properties for $[GeV_{14}O_{40}]^{8-}$; however, it is paramagnetic.

Using the complete set of microscopic interaction intensity evaluated from the ab initio embedded fragment calculation, we have studied the magnetic properties of the compound from the model Hamiltonian suited to represent the whole $[GeV_{14}O_{40}]^{8-}$ anion. A new program (MV-MAGPACK) has been developed to build the matrix representative of the Hamiltonian, to diagonalize it, and to provide its eigenenergies and eigenstates.[32] Then, the density matrices are calculated for each state. For a given eigenstate, the diagonal elements are the electronic population of each orbital, the extra-diagonal elements indicate, for a given position of one electron, the position of the other one. These matrices are very useful to shed some light on the origin of the paramagnetic coupling of the two electrons and emphasize the differences from other POMs.

The singlet-to-triplet energy difference obtained from the diagonalization of the model Hamiltonian is almost zero (0.02 meV), in agreement with experiments. The density matrices of the lowest singlet and triplet states are very similar, and consequently the electronic population (see Table 3). They show a large occupation of each V_4 ion by the "extra" electrons (0.87) and that the electrons remain far from each other: the configurations where the electrons are on each V_4 ion have a weight of 87%, the other 13% of the wave functions come from configurations with one electron on a V_4 ion an the other on a V_1 or V_2 ion at the other half of the compound. All the other configurations contribute to less than 3×10^{-3}%. At this stage, the difference between $GeV_{14}O_{40}$ and $PW_{12}O_{40}$, $W_{10}O_{32}$, or $V_{18}O_{42}$ is not clear, since in any case similar intensity of the microscopic parameters is observed.

The crucial point concerns the peculiar role of the V_3 ions. Indeed, as these ions have two apical oxygen atoms ($d_{V-O} \approx 1.70$ Å), their orbital energy, ε, is much higher than that of the other V ions. Then, the 4-V_3 square forms a barrier between the two pyramidal halves of the compound. Moreover, the other pathways that could link the two halves are weak (see the values of t and J for fragments V_1^l–V_1^r, V_2^l–V_2^r, and V_1^l–V_2^r in Tables 1 and 2). Finally, the V_4 ions have the lowest orbital energy and the Coulombic repulsion is the smallest when the two electrons are on one V_4 each. The most stable configurations are those in which the electrons are each located on a separate V_4. Therefore, delocalization of the electrons between the two halves of the compound is strongly prevented, the two electrons are almost trapped one on each half of the POM (see Figure 2). The resulting effective magnetic interaction is therefore weak, and the compound is paramagnetic. This result is in complete agreement with the conclusions in ref.[14] based on a BVS analysis.

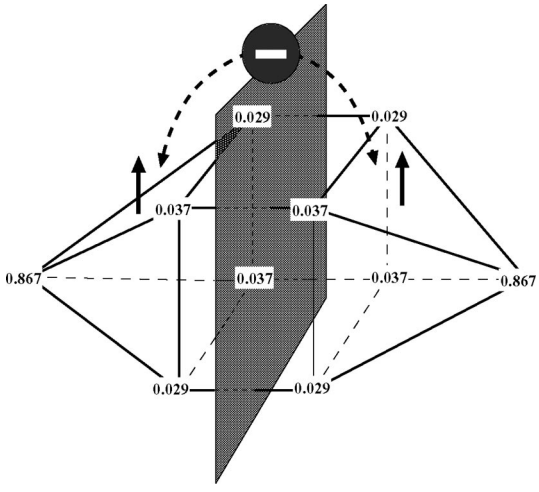

Figure 2. Electron population of the lowest singlet and triplet states of the two-electron-reduced $[GeV_{14}O_{40}]^{8-}$ POM. This result shows that the two "extra" electrons are trapped on each side of the POM molecule as the electron transfer between the two moieties is forbidden.

5 Conclusion

In this paper we have provided an explanation of the origin of the paramagnetic properties of the $[GeV_{14}O_{40}]^{8-}$ anion. It has been shown that the paramagnetic behavior is a consequence of the partial trapping of the two delocalized electrons, in such a way that each unpaired electron is almost trapped on a different half of the polyoxovanadate. Indeed, the electronic structure of the lowest energy singlet and triplet states is dominated by the orbital energy of the metal sites, ε_i, and by the electrostatic interactions between the two extra electrons when they are located on different metal sites, V_{ij}. These parameters have their lowest energy when each "extra" electron is localized on a different half of the POM. Consequently, neither the electron transfer nor the superexchange mechanisms can play any important role. These two degrees of freedom are like frozen in such a way that the effective spin coupling between the two electrons is almost zero.

This result opens the possibility of controlling the spin coupling between the two electrons by applying, for example, an external electrical field. In fact, the effect of a field applied parallel to the main axis of the POM should be to overcome the energy barrier that maintains the electrons trapped on each side, thus favoring the antiferromagnetic coupling between the two spin electrons. This is the aim of a forthcoming paper.

Acknowledgments

We thank Alain Gellé and Marie-Bernadette Lepetit for their Boys localization program, Carmen Jiménez-Calzado for her Effective Hamiltonian extraction program. We thank the computational center IDRIS/CNRS (Paris), where the calculations were performed under project no. 1104. We acknowledge financial support from the European Union (NoE MAGMANet and Project MolSpinQIP), the Spanish Ministerio de Ciencia y Tecnología (Projects MAT-2007-61584 and Consolider-ingenio in Molecular Nanoscience) and the Generalitat Valenciana (PROMETEO Program). The work

in France has been supported by the Centre National de la Recherche Scientifique (CNRS), the "Université de Toulouse", and the Project GDR "Magnétisme et Commutation Moléculaire".

[1] M. T. Pope, A. Müller, *Angew. Chem. Int. Ed. Engl.* **1991**, *30*, 34.
[2] I. V. Kozhevnikov, *Chem. Rev.* **1998**, *98*, 171; N. Mizuno, M. Misono, *Chem. Rev.* **1998**, *98*, 199; M. Sadakane, E. Steckhan, *Chem. Rev.* **1998**, *98*, 219.
[3] J. T. Rhule, C. L. Hill, D. A. Judd, R. F. Schinazi, *Chem. Rev.* **1998**, *98*, 327.
[4] A. Müller, F. Peters, M. T. Pope, D. Gatteschi, *Chem. Rev.* **1998**, *98*, 239; E. Coronado, C. J. Gómez-García, *Chem. Rev.* **1998**, *98*, 273; W. G. Klemperer, C. G. Wall, *Chem. Rev.* **1998**, *98*, 297; J. J. Borrás, E. Coronado, A. Müller, M. T. Pope, *Polyoxometalate Molecular Science, NATO ASI Series II. Mathematics, Physics and Chemistry Vol. 98*, Kluwer Academic Publishers, Dordrecht, **2003**.
[5] J. Lehmann, A. Gaita-Ariño, E. Coronado, D. Loss, *Nature Nanosci.* **2007**, 312; J. Lehmann, A. Gaita-Ariño, E. Coronado, D. Loss, *J. Mater. Chem.* **2009**, *19*, 1672.
[6] J. M. Clemente-Juan, E. Coronado, *Coord. Chem. Rev.* **1999**, *193–195*, 361.
[7] N. Casañ-Pastor, P. Gomez-Romero, G. B. Jameson, L. C. W. Baker, *J. Am. Chem. Soc.* **1991**, *113*, 5658.
[8] M. T. Pope, *Isopoly and Heteropoly Metalates*, Springer-Verlag, Berlin, **1983**.
[9] M. Kozik, C. F. Hammer, L. C. W. Baker, *J. Am. Chem. Soc.* **1986**, *108*, 2748; M. Kozik, L. C. W. Baker, *J. Am. Chem. Soc.* **1987**, *109*, 3159; M. Kozik, N. Casañ-Pastor, C. F. Hammer, L. C. W. Baker, *J. Am. Chem. Soc.* **1988**, *110*, 1697; M. Kozik, L. C. W. Baker, *J. Am. Chem. Soc.* **1990**, *112*, 7604; N. Casañ-Pastor, L. C. W. Baker, *J. Am. Chem. Soc.* **1992**, *114*, 10384.
[10] S. A. Borshch, B. Bigot, *Chem. Phys. Lett.* **1993**, *212*, 398.
[11] J. J. Borrás-Almenar, J. M. Clemente-Juan, E. Coronado, B. S. Tsukerblat, *Chem. Phys.* **1995**, *195*, 1; J. J. Borrás-Almenar, J. M. Clemente-Juan, E. Coronado, B. S. Tsukerblat, *Chem. Phys.* **1995**, *195*, 16.
[12] N. Suaud, A. Gaita-Ariño, J. M. Clemente-Juan, J. Marín-Sánchez, E. Coronado, *J. Am. Chem. Soc.* **2002**, *124*, 15134; N. Suaud, A. Gaita-Ariño, J. M. Clemente-Juan, J. Marín-Sánchez, E. Coronado, *Polyhedron* **2003**, *22*, 2331; N. Suaud, A. Gaita-Ariño, J. M. Clemente-Juan, E. Coronado, *Chem. Eur. J.* **2004**, *10*, 4041; J. M. Clemente-Juan, E. Coronado, A. Gaita-Ariño, N. Suaud, *J. Phys. Chem. A* **2007**, *111*, 9969.
[13] C. J. Calzado, J. M. Clemente-Juan, E. Coronado, A. Gaita-Ariño, N. Suaud, *Inorg. Chem.* **2008**, *47*, 5889.
[14] L.-H. Bi, U. Kortz, M. H. Dickman, S. Nellutla, N. S. Dalal, B. Keita, L. Nadjo, M. Prinz, M. Neumann, *J. Cluster Sci.* **2006**, *17*, 143.
[15] H. T. Evans Jr, J. A. Konnert, *Am. Mineral.* **1978**, *63*, 863.
[16] A. Müller, J. Döring, M. I. Khan, V. Wittneben, *Angew. Chem. Int. Ed. Engl.* **1991**, *30*, 210.
[17] M. E. Thompson, C. H. Roach, R. Meyrowitz, *Amer. Mineral.* **1958**, *43*, 749.
[18] M. T. Pope, *Prog. Inorg. Chem. Vol. 39*, **1991**, p. 181 ; M. T. Pope, A. Müller, *Angew. Chem.* **1991**, *103*, 56; M. T. Pope, A. Müller, *Angew. Chem. Int. Ed. Engl.* **1991**, *30*, 34.
[19] H. Duclusaud, S. A. Borshch, *J. Am. Chem. Soc.* **2001**, *123*, 2825; J. M. Maestre, X. Lopez, C. Bo, J.-M. Poblet, N. Casañ-Pastor, *J. Am. Chem. Soc.* **2001**, *123*, 3749; X. López, J. M. Maestre, C. Bo, J.-M. Poblet, *J. Am. Chem. Soc.* **2001**, *123*, 9571; X. López, J. A. Fernandéz, S. Romo, J. F. Paul, L. Kazansky, J.-M. Poblet, *J. Comput. Chem.* **2004**, *25*, 1542; D. Kumar, E. Derat, A. M. Khenkin, R. Neumann, S. Shaik, *J. Am. Chem. Soc.* **2005**, *127*, 17712; R. Prabhakar, K. Morokuma, C. L. Hill, D. G. Musaev, *Inorg. Chem.* **2006**, *45*, 5703; A. Bagno, M. Bonchio, J. Autschbach, *Chem. Eur. J.* **2006**, *12*, 8460; W. Guan, L.-K. Yan, Z.-M. Su, E.-B. Wang, X.-H. Wang, *J. Mol. Mod.* **2006**, *12*, 551; F.-Q. Zhang, H.-S. Wu, Y.-Y. Xu, Y.-W. Li, H. Jiao, *Int. J. Quantum Chem.* **2006**, *106*, 1860; J. A. Fernández, X. López, C. Bo, C. de Graaf, E. J. Baerends, J. M. Poblet, *J. Am. Chem. Soc. B* **2007**, *129*, 12244; F. Leroy, P. Miró, J. M. Poblet, C. Bo, J. Bonet Ávalos, *J. Phys. Chem. B* **2008**, *112*, 8591; C. Pichon, A. Dolbecq, P. Mialane, J. Marrot, E. Rivière, M. Goral, M. Zynek, T. McCormac, S. A. Borshch, E. Zueva, F. Sécheresse, *Chem. Eur. J.* **2008**, *14*, 3189; S. Romo, C. de Graaf, J. M. Poblet, *Chem. Phys. Lett.* **2008**, *450*, 391; S. Romo, N. S. Antonova, J. J. Carbo, J. M. Poblet, *Dalton Trans.* **2008**, *38*, 5166.
[20] L. Noodleman, J. G. Norman Jr, *J. Chem. Phys.* **1979**, *70*, 4903; L. Noodleman, *J. Chem. Phys.* **1981**, *74*, 5737; L. Noodleman, E. R. Davidson, *Chem. Phys.* **1986**, *109*, 131; L. Noodleman, C. Y. Peng, D. A. Case, J. M. Mouesca, *Coord. Chem. Rev.* **1995**, *144*, 199; I. de P. R. Moreira, C. J. Calzado, J. P. Malrieu, F. Illas, *Phys. Rev. Lett.* **2006**, *97*, 087003; P. Labèguerie, C. Boilleau, R. Bastardis, N. Suaud, N. Guihéry, J.-P. Malrieu, *J. Chem. Phys.* **2008**, *129*, 154110.
[21] E. Derat, E. Lacôte, B. Hasenknopf, S. Thorimbert, M. Malacria, *J. Phys. Chem. A* **2008**, *112*, 13002.
[22] I. de P. R. Moreira, F. Illas, C. J. Calzado, J. F. Sanz, J. P. Malrieu, N. Ben Amor, D. Maynau, *Phys. Rev. B* **1999**, *59*, 6593.
[23] C. J. Calzado, J. Fernandez Sanz, J. P. Malrieu, F. Illas, *Chem. Phys. Lett.* **1999**, *307*, 102; D. Munoz, F. Illas, I. de P. R. Moreira, *Phys. Rev. Lett.* **2000**, *84*, 1579; C. J. Calzado, J. Fernandez Sanz, J. P. Malrieu, *J. Chem. Phys.* **2000**, *112*, 5158.
[24] MOLCAS Version 7. 2, G. Karlström, R. Lindh, P.-Å. Malmqvist, B. O. Roos, U. Ryde, V. Veryazov, P.-O. Widmark, M. Cossi, B. Schimmelpfennig, P. Neogrady, L. Seijo, *Comput. Mater. Sci.* **2003**, *28*, 222.
[25] J. P. Malrieu, *J. Chem. Phys.* **1967**, *47*, 4555; R. Broer, W. J. A. Maaskant, *Chem. Phys.* **1986**, *102*, 103; J. Miralles, O. Castell, R. Caballol, J. P. Malrieu, *Chem. Phys.* **1993**, *172*, 33; J. Cabrero, N. Ben Amor, C. de Graaf, F. Illas, R. Caballol, *J. Phys. Chem. A* **2000**, *104*, 9983.
[26] CASDI suite of programs. D. Maynau, N. Ben Amor and J. V. Pitarch-Ruiz, University of Toulouse, France, **1999**; N. Ben Amor, D. Maynau, *Chem. Phys. Lett.* **1998**, *286*, 211.
[27] Z. Barandiarán, L. Seijo, *Can. J. Chem.* **1992**, *70*, 409.
[28] C. Bloch, *Nucl. Phys.* **1958**, *6*, 329; J. des Cloizeaux, *Nucl. Phys.* **1960**, *20*, 321.
[29] C. J. Calzado, J. F. Sanz, *J. Am. Chem. Soc.* **1998**, *120*, 1051; N. Suaud, M.-B. Lepetit, *Phys. Rev. B* **2000**, *62*, 402; C. J. Calzado, J. P. Malrieu, *Phys. Rev. B* **2001**, *63*, 214520; N. Suaud, M.-B. Lepetit, *Phys. Rev. Lett.* **2002**, *88*, 056404; C. J. Calzado, J. Cabrero, J. P. Malrieu, R. Caballol, *J. Chem. Phys.* **2002**, *116*, 3985; D. Muñoz, I. de P. R. Moreira, F. Illas, *Phys. Rev. B* **2002**, *65*, 224521; E. Bordas, C. de Graaf, R. Caballol, C. J. Calzado, *Phys. Rev. B* **2005**, *71*, 045108; R. Bastardis, N. Guihéry, N. Suaud, C. de Graaf, *J. Chem. Phys.* **2006**, *125*, 194708; R. Bastardis, N. Guihéry, N. Suaud, *Phys. Rev. B* **2007**, *75*, 132403.
[30] a) S. F. Boys, *Rev. Mod. Phys.* **1960**, *32*, 296; b) S. F. Foster, J. M. Boys, *Rev. Mod. Phys.* **1960**, *32*, 300.
[31] The calculation was performed by using a program developed by Alain Gellé, Ph.D. Thesis, Université Paul Sabatier, France, **2004**.
[32] J. J. Borras-Almenar, S. Cardona-Serra, E. Coronado, J. M. Clemente-Juan, A. V. Palii, B. S. Tsukerblat, *J. Comput. Chem.*, DOI: 10.1002/jcc.21400; J. M. Clemente-Juan, J. J. Borras-Almenar, E. Coronado, A. V. Palii, B. S. Tsukerblat, *Inorg. Chem.* **2009**, *48*, 4557.

Received: August 17, 2009
Published Online: October 22, 2009
Since the publication in Early View, ref.[32] has been updated.

